The Influence of Niobium Supersaturation in Austenite on the Static Recrystallization Behavior of Low Carbon Microalloyed Steels

E.J. PALMIERE, C.I. GARCIA, and A.J. DeARDO

This work describes the effect of Nb supersaturation in austenite, as it applies to the strain-induced precipitation potential of Nb(CN), on the suppression of the static recrystallization of austenite during an isothermal holding period following deformation. Four low carbon steels, microalloyed with Nb, were used in this investigation. Three of the steels had variations in Nb levels at constant C and N concentrations. Two steels had different N levels at constant C and Nb concentrations. The results from the isothermal deformation experiments and the subsequent measurement of the solution behavior of Nb in austenite show that the recrystallization-stop temperature (T_{RXN}) increases with increasing Nb supersaturation in austenite. Quantitative transmission electron microscopy analysis revealed that the volume fraction of Nb(CN) at austenite grain boundaries or subgrain boundaries was 1.5 to 2 times larger than Nb(CN) volume fractions found within the grain interiors. This high, localized volume fraction of Nb(CN) subsequently led to high values for the precipitate pinning force (F_{PIN}). These values for F_{PIN} were much higher than what would have been predicted from equilibrium thermodynamics describing the solution behavior of Nb in austenite.

I. INTRODUCTION

THE thermomechanical processing of microalloyed steel has been employed for some time in the production of plate and sheet material in order to optimize properties such as strength and impact toughness.[1–6] More recently,[7,8] this technology has also been applied to the bar and forging industry with considerable success. The central feature of thermomechanically processed steel is the ultrafine grain size in the final product. This fine grain size is known to cause both high strength and high resistance to brittle fracture by cleavage. While achieving high strength in structural steel is rather straightforward and well understood, achieving fine grain size is a more complex task related to the synergy which exists between the composition of the steel and its processing. It has been shown that the final grain size in pearlite-reduced steels is controlled by the metallurgical condition and transformation temperature of the parent austenite.[9,10] The metallurgical condition of the austenite is comprised of its grain size, composition, and crystalline defects, while the transformation temperature is controlled by the composition and defect structure of the austenite, as well as the cooling rate.[3]

The range in behavior of austenite during hot deformation is exhibited schematically in Figure 1. This figure shows the influence of both deformation temperature (T_ϵ) and amount of strain on the microstructure of statically recrystallized austenite. It can be observed from Figure 1 that for constant deformation variables such as strain, strain rate, and interpass holding time, the austenite microstructure will be completely recrystallized at high deformation temperatures (*i.e.*, when $T \geq T_{95\ pct}$). Multipass hot deformation sequences which end in this regime and where there is a pre-existing pinning force to suppress grain coarsening are entitled recrystallization controlled rolling (RCR) practices. Hence, the distinguishing feature of RCR processing is having a pre-existing pinning force (precipitate or solute) that is small enough to allow for static recrystallization to occur but large enough to suppress grain coarsening.

As the deformation temperature is decreased ($T_{95\ pct} > T > T_{5\ pct}$) such that the progress of recrystallization becomes increasingly difficult, a partially recrystallized microstructure is observed. This microstructure is often referred to as being duplex because of a nonuniform grain size. Finally, a completely unrecrystallized microstructure is present when deformation occurs below the recrystallization-stop temperature of austenite, T_{RXN} (*i.e.*, when $T \leq T_{5\ pct}$). Multipass hot deformation sequences which occur largely in this regime are entitled conventional controlled rolling (CCR) practices. For a fixed rolling schedule which includes a specific number of roughing and finishing passes, the higher the T_{RXN}, the larger will be the amount of rolling strain imparted in the nonrecrystallization region. Earlier work[3] has shown that the density of the near-planar crystalline defects (*i.e.*, grain boundaries, deformation bands, and twin boundaries), labeled S_v, increases with increasing deformation in the nonrecrystallization region. Since these defects act as nucleation sites for proeutectoid ferrite during subsequent cooling, there is a strong relationship between the final ferrite grain size and S_v.[11,12,13] The addition of microalloying elements such as niobium, titanium, and vanadium is known to increase T_{RXN}, with niobium having the strongest effect per atomic percent addition.[11] Hence, niobium bearing steels with high T_{RXN} and high S_v values are known to have a very fine ferrite grain size.

Despite nearly 30 years of research, controversy still remains concerning how the microalloying elements act to increase the T_{RXN}. In particular, the basic question remains

E.J. PALMIERE, Assistant Professor, C.I. GARCIA, Associate Research Professor, and A.J. DeARDO, Professor, are with the Department of Materials Science and Engineering, University of Pittsburgh, Pittsburgh, PA 15261.

Manuscript submitted October 1, 1993.

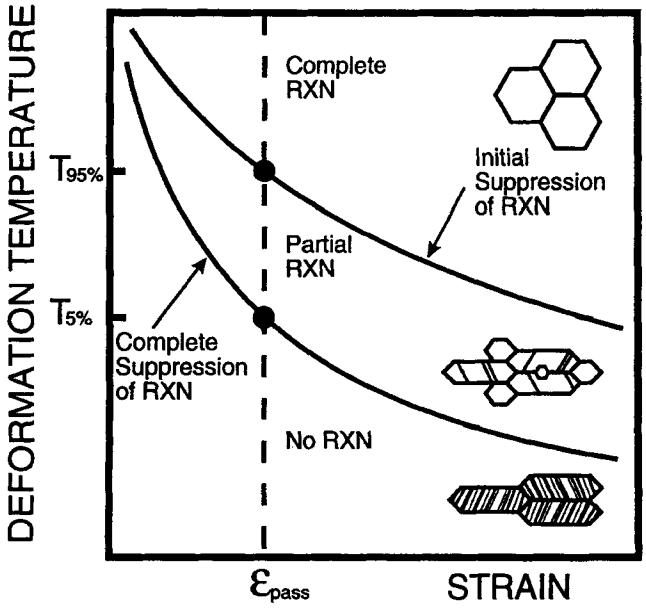

Fig. 1—Schematic illustration of austenite microstructures resulting from various deformation temperatures (T_e) at a constant level of strain.

Table I. Comparison of Expressions for Both N_s and F_{PIN} from Each Precipitate Pinning Force Model

Model	N_s*	F_{PIN}*	Reference
Rigid boundary (R)	$\frac{3f_v}{2\ \pi r^2}$	$\frac{6\sigma f_v}{\pi r}$	37
Flexible boundary (F)	$\frac{3f_v^{2/3}}{4\ \pi r^2}$	$\frac{3\sigma f_v^{2/3}}{\pi r}$	11, 38
Subgrain boundary (S)	$\frac{3f_v\ell}{8\ \pi r^3}$	$\frac{3\sigma f_v\ell}{2\ \pi r^2}$	19

* f_v = precipitate volume fraction; and ℓ = average subgrain boundary intercept distance.

as to how the microalloying elements act to retard the static recrystallization of austenite that would otherwise occur in plain carbon steels during the interpass holding times. Theories involving solute drag[14–18] and precipitate pinning[11,12,19–25] mechanisms have been proposed. The purposes of this present study are to investigate the magnitude of the pinning forces developed by strain-induced precipitation and to compare this pinning force with the magnitude of the driving force causing recrystallization.

A. *Driving Force for Recrystallization*

Microscopic examination has revealed that sites favored for recrystallization nuclei include grain boundaries, phase interfaces, twin boundaries, deformation bands, and the surface of the material.[26] A widely accepted mechanism for the nucleation of recrystallization is the strain-induced boundary migration model.[26–32] This model, which is applicable for low amounts of strain, was originally put forth by Beck and Sperry[30,31] and was subsequently advanced through the work of Bailey and Hirsch.[32] In this model, the driving force for recrystallization is the difference in volume strain energy (*i.e.*, dislocation density) between adjacent austenite subgrains.[26] This model proposes that austenite grains of low dislocation density will "bulge" into grains of high dislocation density.[29] Quantitatively, the driving force for recrystallization (F_{RXN}) based on this model can been described by[28–32]

$$\mathbf{F}_{RXN} = \frac{\mu \mathbf{b}^2 \Delta\rho}{2} \qquad [1]$$

where μ is the shear modulus of austenite, **b** is the Burgers vector, and $\Delta\rho$ is the change in dislocation density associated with the migration of the recrystallization front into the deformed region. Although Eq. [1] shows no direct temperature dependence, it will be indirectly influenced by temperature through the $\Delta\rho$ term. With increasing temperature, $\Delta\rho$ will become smaller due to a number of factors, including an increasing number of operative slip systems and more extensive dynamic softening.[33,34] Hence, the F_{RXN} will decrease to some degree with increasing temperature.

B. *Precipitate Pinning Force Models*

Investigations regarding the retarding effects of second-phase particles on a migrating grain boundary can be traced back to the 1940s, with the original work by Zener.[35] He postulated that when particles were present in the vicinity of a grain boundary, the effective grain boundary energy would be lowered. This reduction in grain boundary energy occurs because the surface area of the second-phase particles effectively replaces a portion of the grain boundary. Therefore, the motion of a grain boundary away from particles would require work due to an effective increase in grain boundary area.[36] This original work was later expanded[37] to consider the motion of grain boundaries through a regular array of particles per unit area (N_s). Hence, the total precipitate pinning force (F_{PIN}) that an array of particles of radius r exerted on a migrating boundary was expressed as

$$F_{PIN} = 4\ r\sigma N_s \qquad [2]$$

where σ is the interfacial energy per unit area of boundary.

From this early work, three models were postulated to explain how microalloy precipitates could suppress austenite recrystallization.[11,19,37,38] The resulting expressions from each model are presented in Table I. Although each model presented in Table I is based upon the general form of Eq. [2], they differ from one another by the method by which N_s is calculated. The rigid boundary model defined N_s through the assumption that the motion of a rigid grain boundary is capable of interacting only with those particles lying within $\pm r$ of the boundary plane.[37] In contrast, the flexible boundary model defined N_s by assuming that an infinitely flexible boundary was capable of interacting with every particle of radius r within a single plane of a three-dimensional array until fully pinned.[11,38] The subgrain boundary model is the most recent and considered the effect of a precipitate distribution which could exist on austenite subgrain boundaries prior to the start of recrystallization.[19]

Austenite recrystallization will be suppressed by microalloy precipitates when $F_{PIN} > F_{RXN}$. In general, order of magnitude calculations based on Eq. [1] and the expressions shown in Table I showed that the difference between F_{PIN} and F_{RXN} was not large.[11,19] Hence, these precipitate pinning force models indicated recrystallization would not be completely suppressed, whereas high resolution micros-

Table II. Steel Compositions in Weight Percent

Element	Composition in Weight Percent				
	E0	E1	E2	E3	E4
C	0.090	0.090	0.080	0.080	0.080
Mn	1.490	1.490	1.470	1.440	1.430
P	0.009	0.009	0.009	0.008	0.010
S	0.006	0.012	0.006	0.006	0.006
Si	0.410	0.410	0.410	0.400	0.290
Nb	—	0.049	0.048	0.020	0.090
N	0.008	0.008	0.024	0.008	0.008

copy studies[21,23,24,39,40] have shown otherwise (*i.e.*, indicative of a situation where $F_{PIN} > F_{RXN}$).

The failure of these models to predict an adequately large F_{PIN} has been rationalized by some investigators[23] by the idea that a high volume fraction of precipitates beyond the resolution of previous transmission electron microscopy studies may be present. Therefore, a large number of fine precipitates with small interparticle spacings would lead to a higher F_{PIN}. In addition, others[22,24] have speculated that perhaps a higher than expected volume fraction of precipitate may be concentrated in the vicinity of the potentially migrating subgrain boundary. The assumption of a uniform distribution of particles was inherent in each model because of the incorporation of equilibrium thermodynamics in the form of solubility products which employed bulk compositions. From the solubility products, precipitate volume fractions were calculated for a given deformation temperature. However, if a uniform particle distribution is assumed, the volume fraction of precipitate at the austenite subgrain boundary, where the precipitate would be most effective in retarding recrystallization, would be identical to the volume fraction throughout the bulk matrix.

Some investigations,[20,23,24] incorporating electron microscopy, have shown the distribution of Nb(CN) precipitation to be localized, showing increased numbers of particles on what appear to be prior-austenite grain boundaries, subgrain boundaries, and deformation bands. In light of these investigations, it has been postulated[24] that prior to the precipitation of Nb(CN), there may be a segregation of solutes toward these microstructural inhomogeneities in austenite. Upon precipitation, a higher localized volume fraction of Nb(CN) would yield a higher pinning force than those previously calculated assuming a uniform initial solute and subsequent particle distribution.

The goal of this research program was to measure the F_{PIN} resulting from a volume fraction of Nb(CN) localized around austenite grain or subgrain boundaries. This pinning force is subsequently related to the experimentally measured solute supersaturation of Nb in austenite.

II. EXPERIMENTAL PROCEDURE

This investigation involved the use of a series of low carbon, silicon-killed laboratory-melted steels having compositions as shown in Table II. Details regarding the choice of steel composition and their primary processing are described elsewhere.[41] Four grades of steel (E1 through E4) microalloyed with niobium were developed based on the reference steel E0. Three of these steels (E1, E3, and E4) displayed similar nitrogen levels with varying niobium concentrations. The fourth steel (E2) displayed a Nb level similar to that of steel E1 but contained 3 times the nitrogen concentration. Hence, using any of the existing solubility relations for Nb(CN) in austenite or other direct experimental techniques,[25,41] these steels should display three different forms of Nb solution behavior in austenite. Consequently, if similar reheating and deformation temperatures are employed, each steel would be expected to have a different Nb supersaturation at any given temperature. Since the Nb supersaturation in austenite is directly related to the driving force for precipitation, these steels should yield evidence as to the role of precipitate supersaturation in the suppression of austenite recrystallization through the formation of strain-induced precipitation.

Static Softening Studies

Isothermal hot compression studies were conducted using an MTS-458 unit modified[42] for deformation under constant true strain rate conditions. Compression specimens consisted of right circular cylinders having a height of 19.1 mm and a diameter of 12.7 mm. Initially, compression specimens were encapsulated in quartz tubes and backfilled with argon. A two-stage reheating cycle involving both a box furnace and a clam-shell, radiation furnace mounted on the upper frame of the MTS was used. The encapsulated specimens were austenitized in the box furnace at 1250 °C for 1 hour. Immediately following this soak time, specimens were water quenched in an iced brine bath so that the microstructure of the austenite at 1250 °C could be retained.

Within the radiation furnace of the MTS unit, specimens were again reheated to 1250 °C and held for 3 minutes. Prior to the placement of specimens between the dies of the compression unit, both the upper and lower surfaces of each specimen were coated with a water-based glass lubricant used to minimize adverse friction effects.

Following the 3-minute reheat at 1250 °C, each specimen was forced air cooled at a rate of ≈30 °C/s to one of the five possible temperatures at which point deformation was immediately commenced. The five deformation temperatures (1100 °C, 1050 °C, 1000 °C, 950 °C, and 900 °C) used in this study are typical of those employed in the plate-rolling industry. Similarly, the deformation parameters, $\varepsilon_1 = \varepsilon_2 = 0.3$, delay time $\equiv t_D = 10$ s, and $\dot{\varepsilon} = 10\ s^{-1}$, are typical of industrial plate-rolling practice.

The deformation sequence described previously is commonly referred to as a "double-hit" test[24] and was designed to measure the overall fractional softening of austenite under the prescribed delay time of 10 seconds. The fractional softening of austenite was measured for each deformation condition based upon the area calculated beneath the flow curves. The details of this technique have been described elsewhere.[24,25,43] At this point, it should be stated that both the hot flow curves and the microstructures of the as-deformed and quenched specimens indicated that dynamic recrystallization did not occur for any of the steels tested at a strain rate of 10 s^{-1}. Under these test conditions, dynamic recrystallization was not observed even for the highest deformation temperature of 1100 °C. This is noteworthy in that the following results will exclusively be a measure of austenite softening or hardening by static or interpass events such as recovery, recrystallization, and precipitation.

Quantitative optical microscopy was performed on all steels to measure the prior-austenite grain size and austenite grain aspect ratio. This was done to complement the mechanical softening data. Additionally, quantitative electron microscopy was performed on carbon extraction replicas to determine the size and volume fraction of Nb(CN) precipitates. These studies were confined to steels E3 and E4 after isothermal compression at various temperatures. The regions of interest for both of these steels were the austenite grain boundaries and grain interiors. Particle size measurements were performed on at least 50 particles for each condition. The volume fraction of particles was calculated according to the method of Ashby and Ebeling[44] and Kelly.[45]

III. RESULTS AND DISCUSSION

A. *Recrystallization-Stop Temperature of Austenite*

The percent fractional softening for all steels is shown in Figure 2. It is apparent that for each steel, the amount of fractional softening observed within the 10-second holding time decreased with decreasing temperature. In fact, all steels except E0 and E3 exhibited fractional hardening at the lowest deformation temperature of 900 °C. It is important to note that since the amount of fractional softening was measured from mechanical testing data, this softening corresponds to the total net softening of austenite during the 10-second delay. Hence, the total softening would be comprised of all static events: softening due to recovery and recrystallization plus hardening due to precipitation. However, since the stacking fault energy of austenite is relatively low (75 mJ/m^2), softening attributed to recovery processes would be limited because of the difficulty for dislocations to cross-slip or climb.[46] Therefore, the overall fractional softening, as depicted in Figure 2, would largely be expected to reflect the softening due to static recrystallization. In fact, previous work[13,14,15] has shown that static recovery processes may comprise anywhere from 15 to 20 pct of the overall softening behavior of austenite.

Employing the criterion that 20 pct of the overall softening is due to recovery, the T_{RXN} for each steel can readily be obtained from Figure 2. All softening greater than 20 pct can be attributed to static recrystallization. As the deformation temperature increases and particles begin to coarsen and possibly go into solution, accelerated recrystallization kinetics are observed.[24] Therefore, the convergence of the curves in Figure 2 above 85 pct fractional softening is indicative of complete recrystallization for the delay time of 10 seconds. Hence, recrystallization-stop temperatures (temperatures corresponding to $T_{5\ pct}$, Figure 1) of 942 °C, 971 °C, 999 °C, and 1030 °C were obtained for steels E3, E1, E2, and E4. The results shown in Figure 2 are unique in that the fractional softening of austenite is measured as a function of deformation temperature at a constant delay time. The delay time of 10 seconds was chosen to represent plate-processing conditions. However, delay times of 1 or 100 seconds could have also been selected to represent a strip-rolling or open-die forging operation, respectively.

The fractional softening data shown in Figure 2 were further complemented using quantitative metallography. This was necessary to verify the correspondence between

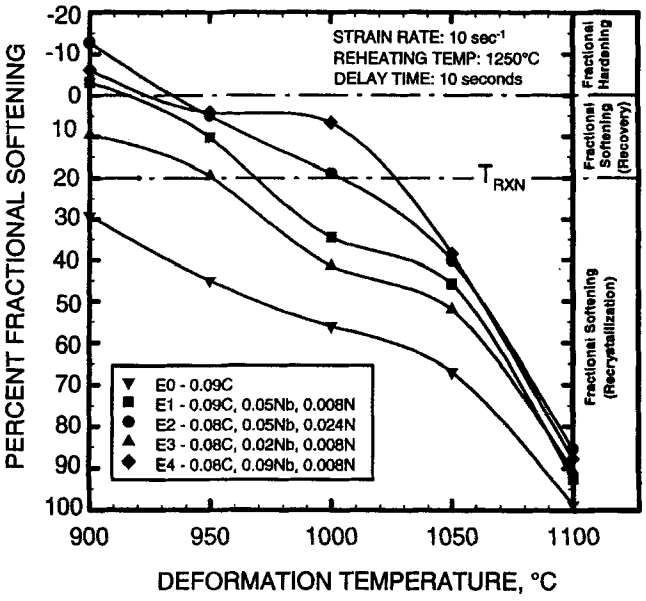

Fig. 2—Percent fractional softening of austenite as determined from interrupted compression testing.

20 pct fractional softening and T_{RXN}. All steels showed good agreement between microstructure and mechanical softening data. At temperatures below the respective T_{RXN} (corresponding to the temperature where 20 pct fractional softening was measured after a 10-second holding time) for each steel, prior-austenite grains are completely unrecrystallized. These grains were elongated in a direction which was perpendicular to the axis of compression. This behavior can be observed for the series of microstructures represented in Figure 3 for steel E4. The T_{RXN} for steel E4 was measured as 1030 °C from interrupted compression testing. The microstructure corresponding to a deformation temperature of 1000 °C indicates completely unrecrystallized prior-austenite grains. The microstructure corresponding to 1050 °C exhibits a predominantly recrystallized microstructure. However, the appearance of unrecrystallized grains can also be detected at 1050 °C. At the next highest deformation temperature of 1100 °C, a completely recrystallized microstructure is observed. The sequence of microstructures for steel E4 suggests that the temperature range ($T_{95\ pct} > T > T_{5\ pct}$) where partial recrystallization can occur is narrow. This temperature range is no greater than 70 °C for any of the steels tested (*i.e.*, $T_{95\ pct} - T_{5\ pct} \leq 70$ °C). In fact, the austenite grain aspect ratios shown in Figure 4 indicate that this temperature range lies between 30 °C and 70 °C, depending on the steel composition. This temperature was determined from the point where the curves deviated from an aspect ratio of unity. Note that at the highest deformation temperature, all steels have aspect ratios which are approximately 1.05, signifying a fully recrystallized microstructure. Similarly, each steel has a comparative aspect ratio (≈2.35) at 900 °C resulting from identical amounts of deformation below the T_{RXN}.

At intermediate deformation temperatures, the variation in aspect ratio is easily observed. It is noteworthy that for each steel, the suppression of recrystallization (*e.g.*, T_{RXN}) corresponded to an aspect ratio between 1.5 to 1.7. This was supported by both the mechanical softening data and quantitative metallography.

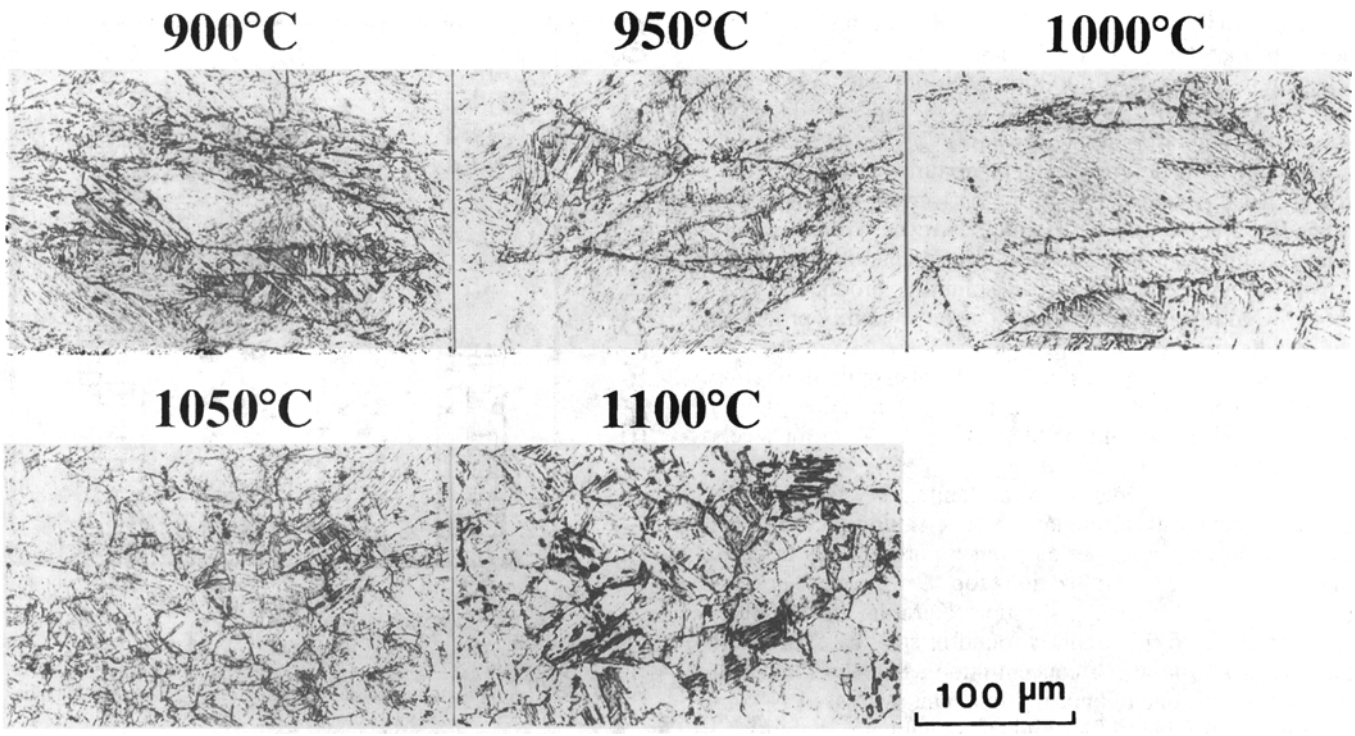

Fig. 3—Microstructure of steel E4 at respective deformation temperatures. Microstructures were obtained after reheating to 1250 °C and interrupted compression testing at a strain rate of 10 s^{-1}. This steel had a T_{RXN} of 1030 °C as measured from static softening studies.

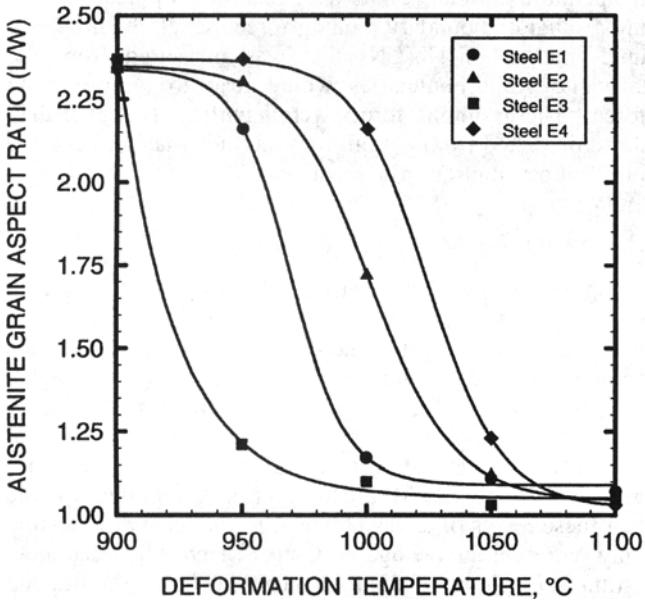

Fig. 4—Austenite grain aspect ratio of microalloyed steels *vs* deformation temperature.

Table III. Niobium Supersaturation in Austenite as a Function of Deformation Temperature[41]

Deformation Temperature (°C)	Nb Supersaturation (Wt Pct · 100)			
	E1	E2	E3	E4
900	4.52	3.86	2.00	7.63
950	4.26	3.38	1.82	6.81
1000	3.32	2.86	1.20	5.23
1050	2.44	2.30	0.63	4.04
1100	1.62	1.66	0.10	3.23

In a related investigation,[25,41] the amount of Nb in solution in austenite was experimentally determined using atom probe analysis. Using these data, it was possible to determine the Nb supersaturation in austenite, $[Nb]_{ss}$, using the relation

$$[Nb]_{ss} = [Nb]_{\gamma} - [Nb]_{\varepsilon} \quad [3]$$

where the terms $[Nb]_{\gamma}$ and $[Nb]_{\varepsilon}$ represent the amount of Nb in solution in austenite at the respective reheating and deformation temperatures. The results of this analysis are shown in Table III for each microalloyed steel. If the fractional softening data and the quantitative metallographic data are combined with the results of Table III, some interesting behaviors can be noted. These results are summarized in Figure 5, which depicts the Nb supersaturation in austenite at the respective T_{RXN} of each steel. Figure 5 shows that the Nb supersaturation at the T_{RXN} varies with each steel and is dependent on the initial steel composition. A similar difference would be observed if the data had been normalized about the respective initial Nb concentration of each steel.

An earlier investigation[19] had suggested that a critical Nb supersaturation must be exceeded for strain-induced Nb(CN) precipitation to retard austenite recrystallization. Furthermore, it was suggested that the suppression of recrystallization was associated with similar Nb supersaturation ratios, where the supersaturation ratio was defined as being the solubility product of Nb(CN) in austenite at the reheating temperature to the solubility product of Nb(CN) in austenite at the deformation temperature. In this previous investigation, the solubility product of Nb(CN) was calculated using the expression of Irvine *et al.*[1] Accordingly, the two steel compositions in this previous investigation exhibited supersaturation ratios of 7.5 and 5 when reheated

to 1250 °C and deformed at 950 °C. It has been shown,[25,41] however, that there is no unique solubility expression which adequately relates the solubility of Nb in austenite for various steel compositions. In fact, Cuddy[11] calculated the Nb supersaturation ratios at the respective T_{RXN} of several steels rather than at the deformation temperature. He subsequently found that the supersaturation ratios were not constant but ranged between 5 and 40. He did, however, express uncertainty in his results because of the calculation of soluble Nb in austenite from published solubility products.[47] Although Cuddy based his calculations on solubility products, the results from his investigation compare favorably with the results of the present study. If Nb supersaturation ratios were calculated from the atom probe data, ratios of 9.3, 6.2, 4.6, and 5.5 would be attained at the T_{RXN} for steels E1, E2, E3, and E4, respectively.

Although the suppression of austenite recrystallization is not associated with a unique Nb supersaturation, an interesting trend can be observed from Figure 5. This trend is that increasing recrystallization-stop temperatures are associated with increasing Nb supersaturation in austenite. The exception to this trend is found in steel E2. This steel had the same initial Nb concentration as steel E1 but had 3 times the nitrogen concentration. This increased N concentration provided for higher precipitate stability.[41] Therefore, at the reheating temperature of 1250 °C, steel E2 had significantly less Nb in solution in austenite than steel E1. Hence, for the same reheating and deformation temperature, steel E2 would have a smaller Nb supersaturation than steel E1. The reason that steel E2 exhibits a higher T_{RXN} than steel E1 is most likely due to an increased amount of undissolved particles in addition to the strain-induced precipitation of Nb(CN).

B. *Quantitative Description of Nb(CN) Dispersions in Austenite*

Transmission electron microscopy studies on steels E3 and E4 revealed a localized distribution of Nb(CN) in austenite. An example of this localized distribution is shown in Figure 6, which is similar to the results found in earlier studies on this form of precipitation.[20,22,24] Figure 6 shows a centered dark-field micrograph depicting Nb(CN) precipitates in steel E4 which was deformed at 10 °C below the T_{RXN} of 1030 °C. It is clear from both of these microstructures that the Nb(CN) precipitates are highly localized. Figure 6 shows evidence of precipitates in close proximity to the remnant of a grain boundary. Quantitative microscopy of this steel at various other deformation temperatures further indicated that the volume fraction of Nb(CN) decreased with increasing deformation temperature. This behavior is illustrated for steel E4 in Figure 7.

The measured data of Figure 7 can further be compared to what would have been predicted from equilibrium thermodynamic calculations, incorporating a mass balance on a Nb(CN) precipitate of fixed stoichiometry. A comparison between this equilibrium volume fraction (EQ) and the experimentally determined volume fraction for steel E4 is shown in Figure 7. In this figure, "B" represents the volume fraction of precipitate at austenite grain boundaries and "M" represents the volume fraction of precipitate in the matrix or grain interiors. It is clear from Figure 7 that the equilibrium volume fraction lies between the experimentally determined volume fractions at austenite grain boundaries and grain interiors. This was true for any deformation temperature. Similar results were recorded for steel E3. Using a subgrain boundary pinning force model, the high volume fraction of Nb(CN) that was measured from the austenite grain boundaries would lead to high pinning forces. These pinning forces were significantly higher than those predicted from equilibrium thermodynamics (and the inherent assumption of a constant N_s).

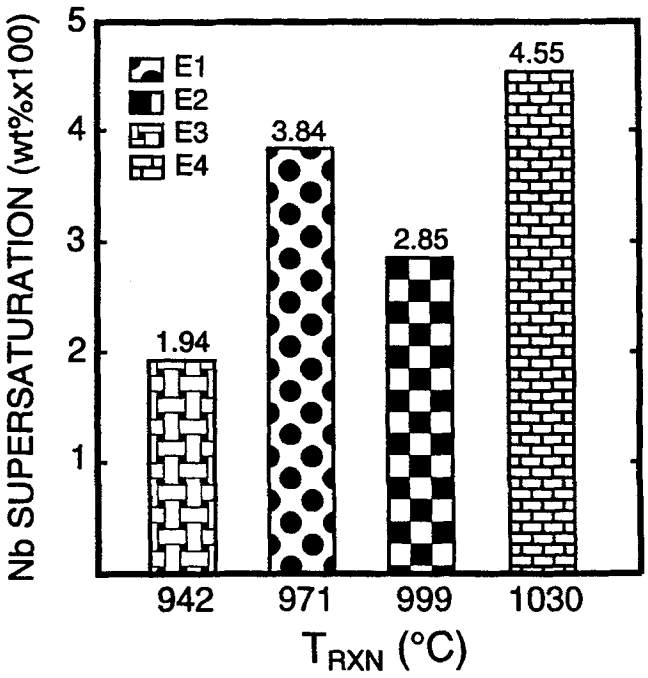

Fig. 5—Nb supersaturation in austenite at the respective recrystallization-stop temperatures for steels E1 through E4.

C. *Relationship between F_{RXN} and F_{PIN}*

Figure 8 shows the variation of both F_{PIN} and F_{RXN} with deformation temperature. The curve for F_{RXN} in Figure 8 was measured using the increase in stress ($\Delta\sigma$) obtained from the flow curve for each steel at a true strain of 0.3 (*i.e.*, the amount of deformation preceding the static delay time). At the extreme deformation temperatures (900 °C and 1100 °C), this respective increase in stress was approximately 205 and 176 MPa. However, it is important to note that these levels of stress obtained from mechanical testing only represent an average flow stress. Hence, to accurately estimate F_{RXN}, one should consider the flow stress at the grain boundaries, which has been approximated to be 50 pct greater than the average flow stress.[48] Therefore, the estimated flow stress at the grain boundaries at 900 °C and 1100 °C is 308 and 264 MPa, respectively. Incorporating Keh's[49] relationship, which relates the increase in dislocation density ($\Delta\rho$) during work hardening to the increase in flow stress,

$$\Delta\sigma = 0.2\ \mu\mathbf{b}\ \sqrt{\Delta\rho} \qquad [4]$$

one can directly calculate the F_{RXN} by the substitution of Eq. [4] into Eq. [1]. This substitution results in

$$F_{RXN} = \frac{12.5\ \Delta\sigma^2}{\mu} \qquad [5]$$

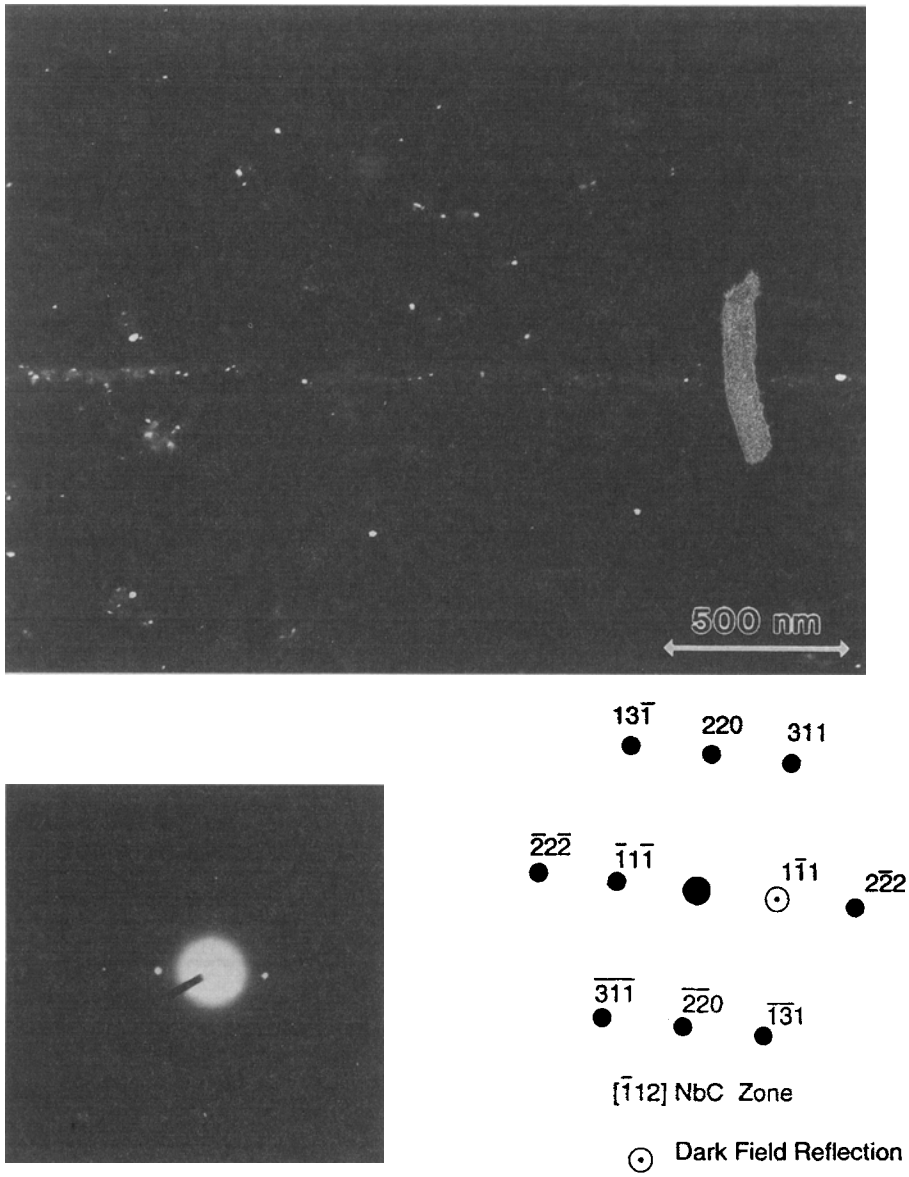

Fig. 6—Extraction replica depicting Nb(CN) precipitation at austenite grain boundary for steel E4. The specimen was reheated to 1250 °C and deformed at 1020 °C, 10 °C below the T_{RXN}. A centered dark-field micrograph was taken from a [111] NbC reflection.

Approximating the shear modulus of austenite (μ) as $4 \cdot 10^4$ MPa,[19] values for F_{RXN} ranged from 22 MN·m^{-2} (at 1100 °C) to 30 MN·m^{-2} (at 900 °C).

The measured pinning forces for steels E3 and E4 showed good agreement with the results from the fractional softening studies and quantitative metallography (Figures 2 and 3). At a deformation temperature of 900 °C, quantitative metallography indicated that the microstructure of both steels E3 and E4 was fully unrecrystallized. This behavior can be explained by the results in Figure 8. At 900 °C, the F_{PIN} for steel E4, calculated at austenite grain boundaries or grain interiors, was larger than the F_{RXN}. At this same temperature, however, steel E3 had a F_{PIN} greater than F_{RXN} only for precipitate volume fractions measured at austenite grain boundaries. This is a reflection of steel E3 having a smaller Nb supersaturation in austenite at 900 °C than steel E4. The precipitation behavior of steel E3 indicates that the suppression of austenite recrystallization is strongly influenced by particles in the vicinity of austenite subgrain or grain boundaries. This behavior is in agreement with the subgrain boundary precipitate pinning model,[19] which assumes that particles are present at austenite grain and/or subgrain boundaries prior to the onset of recrystallization.

At the other extreme in deformation temperature (1100 °C), the F_{PIN} for steels E3 and E4, measured at either the grain boundary or grain interior, is less than the F_{RXN}. This is attributed to the small Nb supersaturation for both of these steels at 1100 °C. However, at this temperature, steel E4 shows a smaller amount of fractional softening than steel E3. This behavior is indicative of solute drag retarding austenite recrystallization at elevated temperatures prior to precipitation events.[16,17,18] Therefore, it is not surprising that steel E4 shows less softening at 1100 °C since it has more Nb in solution in austenite. Finally, the fact that steel E3 had essentially a zero F_{PIN} was a consequence of deformation at a temperature very close to the precipitate solution temperature for steel E3.

At 10 °C below the T_{RXN} of steel E4, the F_{PIN} calculated

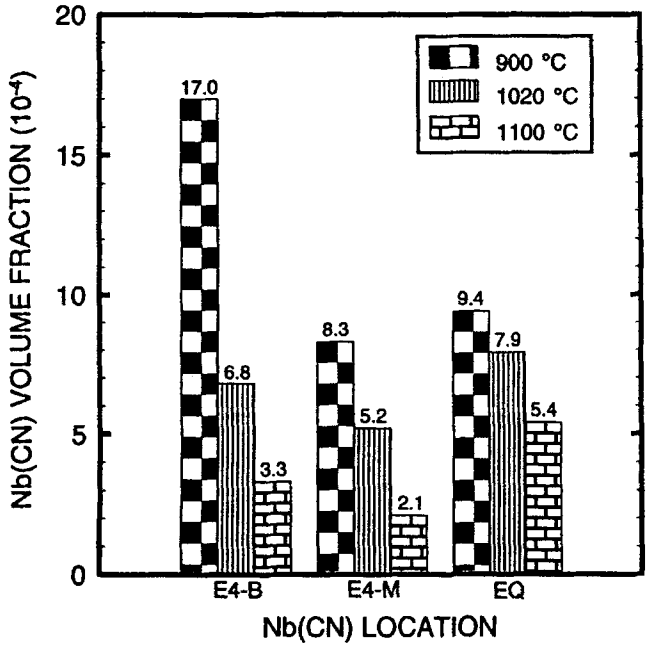

Fig. 7—Nb(CN) volume fraction for steel E4 at austenite grain boundaries (B), within austenite grains (M), and what would be predicted from solubility products (EQ).

Table IV. Comparison of Parameters for Steels E3 and E4 as Measured from This Investigation*

Parameter	E3	E4
T_{RXN} (°C)	942	1030
Aspect ratio at T_{RXN}	1.59	1.74
F_{PIN} in matrix (MN · m^{-2})	19.5	24.9
F_{PIN} at boundary (MN · m^{-2})	30.1	44.9
Bulk Nb concentration (wt pct)	0.020	0.090
Soluble Nb in austenite at 1250 °C (wt pct)	0.020	0.077
Soluble Nb in Austenite at T_{RXN} (wt pct)	0.001	0.031
Nb supersaturation at T_{RXN} (wt pct)	0.019	0.046
Nb supersaturation ratio	4.6	5.5

*The F_{PIN} for steels E3 and E4 was calculated from precipitate measurements on specimens deformed at 12 °C and 10 °C below their respective T_{RXN}.

from the Nb(CN) volume fraction at austenite grain boundaries was approximately 19 MN·m^{-2} greater than the F_{RXN}. In contrast, the F_{PIN} calculated based on volume fractions in grain interiors was ≈1 MN·m^{-2} less than the F_{RXN}. Hence, the average between these two F_{PIN} yields a net pinning force that is 9 MN·m^{-2} greater than the F_{RXN} and corresponds to the static softening and metallographic results. Also, these results are in agreement with other investigations[19,23,28] regarding the precipitation behavior of Nb(CN) in austenite. These studies suggest that the strain-induced precipitation from hot deformed austenite occurs in two stages. First, Nb(CN) precipitation occurs at austenite grain boundaries and deformation bands. This is followed by general matrix precipitation on the substructure of the unrecrystallized austenite. Similar precipitation behavior was also indicated for steel E3 when analyzed at 12 deg below its T_{RXN}. However, the F_{PIN} for steel E3 calculated from a Nb(CN) volume fraction at grain boundaries

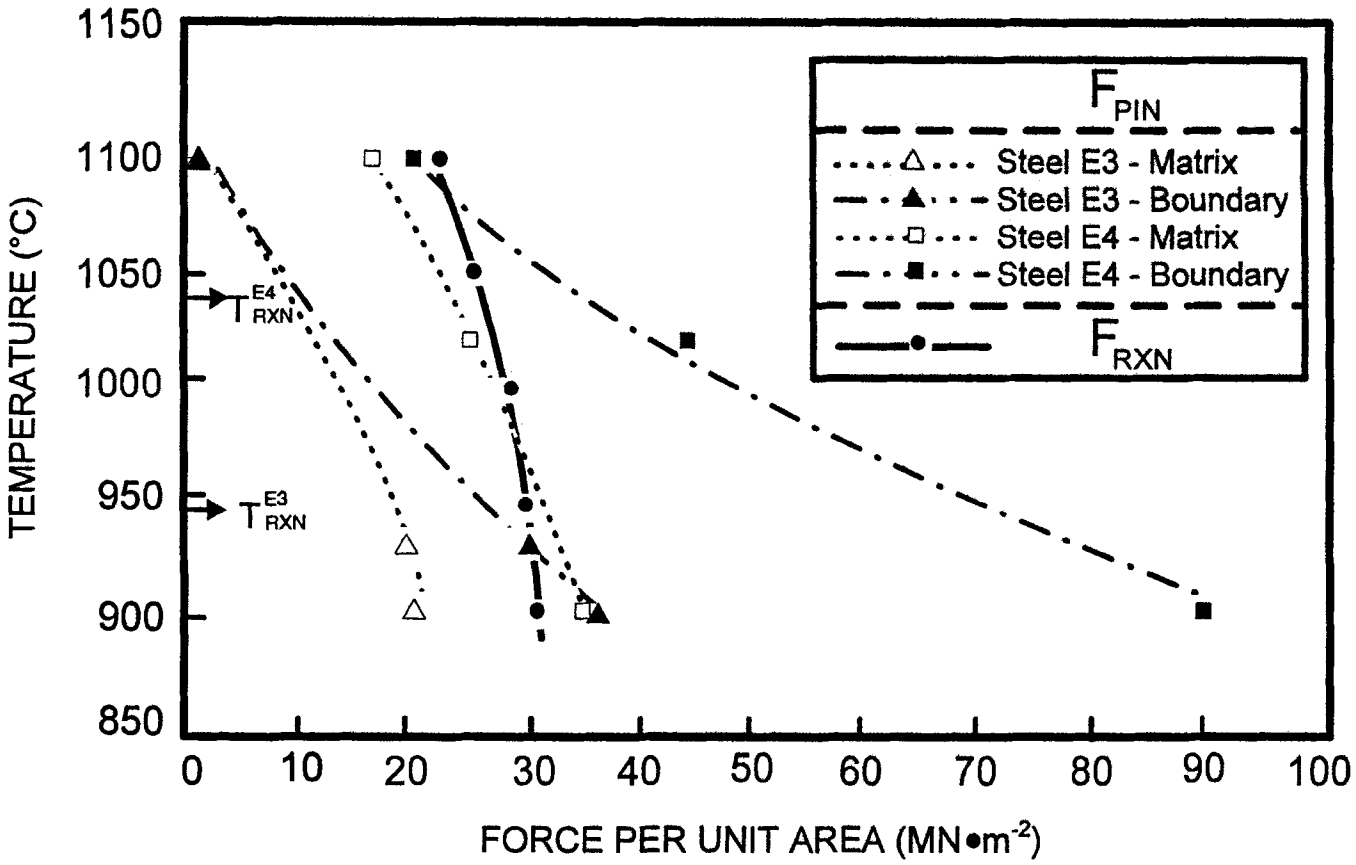

Fig. 8—Comparison between F_{PIN} and F_{RXN} *vs* deformation temperature. Data to the right of F_{RXN} will result in the complete suppression of austenite recrystallization. Data to the left of F_{RXN} will result in a partially or fully recrystallized austenite microstructure.

is of the same magnitude as the F_{RXN}. The reason that a higher F_{PIN} was not calculated for steel E3 is due to the extraction of precipitates on the carbon replicas. The extraction efficiency is always less than 100 pct. Consequently, the calculated values of F_{PIN} serve as a conservative number.

It was mentioned previously that at their respective T_{RXN}, steels E3 and E4 exhibited a different Nb supersaturation in austenite. This is summarized in Table IV along with the calculated values for F_{PIN} at T_{RXN}. Table IV indicates that steel E4 had a Nb supersaturation in austenite which was approximately 2.4 times greater than that of steel E3. However, at their respective T_{RXN}, steel E3 displayed a boundary F_{PIN} that was only 1.5 times smaller than that of steel E4. The average value for F_{PIN} at the T_{RXN} ranged between 25 and 35 $MN \cdot m^{-2}$. Similar values of F_{PIN} for both steels at this temperature resulted from the relatively weak temperature dependence of F_{RXN}. Additionally, although steel E4 had a higher precipitate volume fraction than steel E3, the average particle size measured from steel E4 was greater than that of steel E3.

The particle size measurements previously reported[41] from this investigation correspond with those made from other studies.[22,23] This investigation, along with the others, has shown that the limit of detection for particle diameters when extracted on carbon films is approximately 1 to 2 nm. Additionally, this investigation was able to detect fine scale particles using field ion microscopy (FIM). Similar work was performed by Brenner *et al.*[23] Using measurements from both TEM and FIM, the investigation by Brenner *et al.*[23] related the particle radius and number density (N_v) of precipitate to the occurrence of subgrain boundary pinning. The results from this study and the present investigation are very close, lending further validity to the grain and/or subgrain boundary pinning mechanism.

IV. CONCLUSIONS

The following conclusions can be made regarding the suppression of recrystallization during the hot deformation of microalloyed austenite.

1. Isothermal interrupted compression testing proved to be a relatively easy and reliable method for determining the T_{RXN}. The T_{RXN} was associated with 20 pct of the total fractional softening of austenite. A T_{RXN} of 942 °C, 971 °C, 999 °C, and 1030 °C was measured for steels E3, E1, E2, and E4, respectively.
2. The results from compression studies were verified by quantitative metallography. An austenite grain aspect ratio of 1.5 to 1.7 was measured at the respective T_{RXN} for each steel. Microscopy indicated that below the T_{RXN} for any steel, prior austenite grains were unrecrystallized. At temperatures 30 °C to 70 °C above the T_{RXN}, a fully recrystallized microstructure was present.
3. The coupling of the results from atom probe analysis[41] and the results from interrupted compression testing indicates that the T_{RXN} increases with increasing Nb supersaturation in austenite. This level of Nb supersaturation was not constant from steel to steel.
4. High resolution microscopy on carbon extraction replicas from steels E3 and E4 indicated a high, localized volume fraction of Nb(CN) at prior austenite grain boundaries. The volume fraction of precipitate at the boundary was 1.5 to 2 times higher than the measured volume fraction of Nb(CN) within prior-austenite grains. Additionally, the measured volume fraction of Nb(CN) at austenite grain boundaries or grain interiors was higher than what would have been predicted using existing solubility products for Nb(CN) from the literature. This high volume fraction of Nb(CN) at austenite grain boundaries translated into high values for the precipitate pinning force.
5. The calculated values of F_{PIN} for steels E3 and E4 showed good correspondence with quantitative metallography and fractional softening measurements. This agreement confirms the validity of precipitate pinning along austenite grain and/or subgrain boundaries suppressing austenite recrystallization.
6. The driving force for recrystallization was determined from isothermal compression testing. Values for F_{RXN} were calculated based upon the increase in flow stress prior to the delay time of 10 seconds. At any given temperature, the F_{RXN} was similar for all steels. Although steels E3 and E4 exhibited substantially different Nb(CN) volume fractions (resulting from different Nb supersaturations in austenite) at their respective T_{RXN}, their respective pinning forces were not significantly different. This was attributed to both the smaller particles in steel E3 and the weak dependence of F_{RXN} with temperature.

ACKNOWLEDGMENTS

The authors would like to thank the David Taylor Research Laboratories, the United States Navy, and Niobium Products Corporation, Inc. for the financial support of this research program.

REFERENCES

1. K.J. Irvine, F.B. Pickering, and T. Gladman: *J. Iron Steel Inst.*, 1967, Feb., p. 161.
2. K.J. Irvine: *Low Alloy High Strength Steels*, Nuremberg, The Metallurg Companies, Düsseldorf, 1970, p. 1.
3. I. Kozasu and T. Osuka: in *Processing and Properties of Low Carbon Steel*, J.M. Gray, ed., TMS-AIME, New York, NY, 1973, p. 47.
4. F.B. Pickering: *Microalloying 75*, Washington, DC, M. Korchynsky, ed., Union Carbide Corporation, New York, NY, 1977, p. 9.
5. W.J. McG. Tegart and A. Gittins: *The Hot Deformation of Austenite*, Cleveland OH, J.B. Ballance, ed., TMS-AIME, Warrendale, PA, 1977, p. 1.
6. P.K. Amin and F.B. Pickering: *Thermomechanical Processing of Microalloyed Austenite*, Pittsburgh PA, A.J. DeArdo, G.A. Ratz, and P.J. Wray, eds., TMS-AIME, Warrendale, PA, 1982, p. 1.
7. J.H. Woodhead: *Fundamentals of Microalloying Forging Steels*, Golden CO, G. Krauss and S.K. Banerji, eds., TMS-AIME, Warrendale, PA, 1987, p. 3.
8. C.I. Garcia, E.J. Palmiere, and A.J. DeArdo: *Mechanical Working and Steel Processing Proc.*, Dearborn, MI, Iron and Steel Society, Warrendale, PA, 1989, p. 59.
9. T. Gladman and F.B. Pickering: *J. Iron Steel Inst.*, 1967, June, p. 653.
10. M. Ali Bepari: *Metall. Trans. A*, 1989, vol. 20A, p. 13.
11. L.J. Cuddy: *Thermomechanical Processing of Microalloyed Austenite*, Pittsburgh, PA, A.J. DeArdo, G.A. Ratz, and P.J. Wray, eds., TMS-AIME, Warrendale, PA 1982, p. 129.
12. L.J. Cuddy: *Metall. Trans. A*, 1981, vol. 12A, pp. 1313-20.
13. W. Roberts and B. Ahlblom: *Acta Metall.*, 1978, vol. 26, p. 801.
14. R.A.P. Djaic and J.J. Jonas: *Metall. Trans.*, 1973, vol. 4, pp. 621-24.

15. R.A. Petkovic, M.J. Luton, and J.J. Jonas: *Can. Metall. Q.*, 1975, vol. 14, p. 137.
16. M.J. White and W.S. Owen: *Metall. Trans. A*, 1980, vol. 11A, pp. 597-604.
17. H. Weiss, A. Gittins, G.G. Brown, and W.J. McG. Tegart: *J. Iron Steel Inst.*, 1973, vol. 211, p. 703.
18. M.J. Luton, R. Dorvel, and R.A. Petkovic: *Metall. Trans. A*, 1980, vol. 11A, pp. 411-20.
19. S.S. Hansen, J.B. Vander Sande, and M. Cohen: *Metall. Trans. A*, 1980, vol. 11A, pp. 387-402.
20. M.L. Santella: Ph.D. Thesis, University of Pittsburgh, Pittsburgh, PA, 1981, p. 49.
21. J.G. Speer, J.R. Michael, and S.S. Hansen: *Metall. Trans. A*, 1987, vol. 18A, pp. 211-22.
22. J.G. Speer and S.S. Hansen: *Metall. Trans. A*, 1989, vol. 20A, pp. 25-38.
23. S.S. Brenner, M.G. Burke, L.J. Cuddy, M.K. Miller, and J. Piller: *Proc. 29th Int. Field Emission Symp.*, Göteborg, Sweden, H.-O. Andrén and H. Nordén, eds., Almquist and Wiksell International, Stockholm, 1982, p. 457.
24. O. Kwon and A.J. DeArdo: *Acta Metall.*, 1991, vol. 39, p. 529.
25. E.J. Palmiere: Ph.D. Thesis, University of Pittsburgh, Pittsburgh, PA, 1991, p. 60.
26. R.W.K. Honeycombe: *The Plastic Deformation of Metals*, 2nd ed., ASM, Metals Park, OH, 1984, p. 287.
27. W.C. Leslie: *The Physical Metallurgy of Steels*, McGraw-Hill Book Company, New York, NY, 1981, p. 43.
28. J.W. Martin and R.D. Doherty: *Stability of Microstructure in Metallic Systems*, Cambridge University Press, Cambridge, United Kingdom, 1976, p. 40.
29. R.W. Cahn: *Recrystallization, Grain Growth and Textures*, New York, NY, H. Margolin, ed., ASM, Metals Park, OH, 1966, p. 99.
30. P.A. Beck and P.R. Sperry: *Trans. AIME*, 1949, vol. 185, p. 240.
31. P.A. Beck and P.R. Sperry: *J. Appl. Phys.*, 1950, vol. 21, p. 150.
32. J.E. Bailey and P.B. Hirsch: *Proc. R. Soc. (London)*, 1962, vol. A267, p. 11.
33. A. Kelly and G.W. Groves: *Crystallography and Crystal Defects*, Addison-Wesley Publishing Company, Reading, MA, 1970, p. 198.
34. J.D. Verhoeven: *Fundamentals of Physical Metallurgy*, John Wiley and Sons, New York, NY, 1975, p. 77.
35. C. Zener: *Trans. AIME*, 1949, vol. 175, p. 15.
36. M.F. Ashby: *Recrystallization and Grain Growth of Multi-Phase and Particle Containing Materials: 1st RISO Int. Symp. on Metallurgy and Material Science*, Denmark, N. Hansen, A.R. Jones, and T. Leffers, eds., RISO National Laboratory, Roskilde, Denmark, 1980, p. 325.
37. T. Gladman: *Proc. R. Soc. (London)*, 1966, vol. 294, p. 298.
38. L.J. Cuddy: *Recrystallization and Grain Growth of Multi-Phase and Particle Containing Materials: 1st RISO Int. Symp. on Metallurgy and Material Science*, Denmark, N. Hansen, A.R. Jones, and T. Leffers, eds., RISO National Laboratory, Roskilde, Denmark, 1980, p. 317.
39. J.M. Silcock: *J. Iron Steel Inst.*, 1963, vol. 201, p. 409.
40. A.T. Davenport, L.C. Brossard, and R.E. Miner: *J. Met.*, 1975, vol. 27, p. 21.
41. E.J. Palmiere, C.I. Garcia, and A.J. DeArdo: *Metall. Trans. A*, 1994, vol. 25A, p. 277.
42. G. Fitzsimons, H.A. Kuhn, A.J. DeArdo, and V.M. Sample: *ASTM Symp. Compression Testing of Homogeneous Materials and Composites*, ASTM, Williamsburg, VA, 1982, p. 27.
43. E.J. Palmiere, C.I. Garcia, and A.J. DeArdo: *Int. Symp. on Low-Carbon Steels for the 90's*, R. Asfahani and G. Tither, eds., TMS-AIME, Warrendale, PA, 1993, p. 121.
44. M.F. Ashby and R. Ebeling: *Trans. AIME*, 1966, vol. 236, p. 1396.
45. P.M. Kelly: *Met. Forum*, 1982, vol. 5, p. 13.
46. W. Charnock and J. Nutting: *J. Met. Sci.*, 1967, vol. 1, p. 123.
47. H. Nordberg and B. Aronsson: *J. Iron Steel Inst.*, 1968, Dec., p. 1263.
48. J.P. Hirth: *Metall. Trans.*, vol. 3, 1972, pp. 3047-67.
49. A.S. Keh: *Direct Observation of Imperfections in Crystals*, J.B. Newkirk and J.H. Wernick, eds., Wiley-Interscience, New York, NY, 1962, p. 213.